

Comparison of Dirac and microscopic Schrödinger optical model potentials for nucleon-nucleus scattering

S. Karataglidis and D. G. Madland

Theoretical Division, Los Alamos National Laboratory, Los Alamos, New Mexico, 87545
(October 31, 2018)

Abstract

Detailed comparisons are made between results of calculations for intermediate energy nucleon- ^{208}Pb scattering using optical potentials obtained from Dirac phenomenology and a microscopic Schrödinger model. The two approaches yield quite similar results for all of the observables with each projectile, including spin observables, suggesting the two models are physically equivalent. A new phenomenon in the analyzing power is confirmed in the results for 100 MeV scattering.

24.10.Ht, 21.30.Fe, 25.40.Cm, 25.40.Dn

arXiv:nucl-th/0103048v2 27 Aug 2001

The physics of the interaction of a nucleon with the nucleus has traditionally been represented by the optical potential. Once the optical potential is specified, and thus the scattering matrix, all observables may be calculated. For intermediate energies there have been a number of methods of calculating the optical potential, the most successful of which have been the Dirac phenomenology [1] and a recent microscopic, coordinate space, Schrödinger model [2]. Both approaches have had success in not only predicting differential cross sections, but spin and integral observables as well [2–5]. Note that these models are fundamentally different. The phenomenological Dirac model is dependent on the fitting of data to determine the parameters in the assumed potentials. The microscopic Schrödinger model is derived from the bare nucleon-nucleon (NN) potential to obtain an effective interaction in-medium that when folded with a suitable representation of the target density gives the optical potential. While a Schrödinger-like potential may be derived from the phenomenological Dirac one, there is no *a priori* reason to assume that that nonrelativistic potential resembles in any way the potential obtained from the microscopic model.

Yet no real comparison has been made of the results from the Dirac and microscopic Schrödinger approaches for both projectiles simultaneously. An earlier comparison of the Dirac and phenomenological Schrödinger models showed problems inherent in the latter [3]. The phenomenological Schrödinger model usually assumes a local Woods-Saxon form of the optical potential, whose parameters are determined by fitting a complete set of data. Such an approach generally fails to reproduce the spin observables due to the assumptions made in defining the spin-orbit potential and in the neglect of nonlocality in the potential, arising microscopically from the antisymmetrization of the wave function of the projectile and bound state nucleon in the initial state. The purpose of this Letter is to compare in detail the Dirac phenomenology and microscopic Schrödinger models for both proton and neutron scattering in the energy region in which they have had success. The case we have chosen is that of nucleon elastic scattering from ^{208}Pb at 100–300 MeV. Previous work has been done on this system at this energy range in the Dirac approach [6], from which a striking phenomenon was identified in the analyzing power at 100 MeV: the proton and neutron analyzing powers are exactly out of phase with each other and the one is nearly the inverse of the other about their mean.

The Dirac phenomenology begins with spherically symmetric complex Lorentz isoscalar-scalar and isoscalar-vector potentials together with the Coulomb potential leading to a Walecka-like scattering model [7] with a large attractive scalar potential and an almost as large repulsive vector potential. A second-order reduction of the Dirac equation then leads to a Schrödinger-equivalent equation with physically correct effective central and spin-orbit potentials by which the observables are accurately predicted. The spin-orbit term and a Coulomb correction term (accounting for part of the difference between proton and neutron in-medium projectile motion) appear naturally. Projectile and target isospin dependences are treated by introducing corresponding spherically symmetric complex Lorentz isovector-scalar and isovector-vector potentials in a relativistic generalization of the standard Lane model [8]. The resulting Dirac equation is suitable for simultaneous analyses of proton-nucleus and neutron-nucleus scattering data up to several GeV, provided that the parameters of the potential have been determined by least-squares adjustment to existing experimental data [9,10]. Such was done by Kozack and Madland [6] for nucleon- ^{208}Pb scattering, using energy-independent symmetrized Woods-Saxon form factors, and those results

are reproduced herein.

The microscopic Schrödinger approach [2] does not assume any phenomenological form for the potential nor is it derived from any phenomenological potential. It begins instead with the g matrices of the NN potential; those g matrices are solutions of the Brueckner-Bethe-Goldstone equation in infinite nuclear matter. The Bonn-B NN potential [11] was chosen as the starting point for the calculations presented herein. A local density approximation is used to map the infinite matter solution to the nucleus in question by which an effective NN interaction is defined in medium. When folded with an appropriate ground state density of the target, the microscopic optical potential is obtained naturally, incorporating Pauli blocking and density dependences. The (coordinate space) potential contains both direct and exchange parts, with the exchange terms arising from the antisymmetrization of the projectile and bound state nucleon wave functions, and so the potential is fully nonlocal. There are no parameters in the model which must be adjusted after the fact to achieve a reasonable fit: all results are obtained from a single predictive calculation. We use the code DWBA98 [12] to calculate the optical potential and observables. Success has been achieved predicting the observables from proton-nucleus scattering for a number of nuclei across a range of energies [2]. For the present case, the ground state density for ^{208}Pb was obtained from a Skyrme-Hartree-Fock calculation by Brown [13]. As the g matrix is defined for all two-body spin and isospin channels, the isospin of the projectile selects the correct components of the matrix to define the appropriate optical potential for that projectile. As such the same g matrix defines the optical potentials for both proton and neutron scattering in a natural way. The Coulomb interaction is, of course, also included in the calculations of proton scattering.

In Fig. 1, we compare the differential cross sections for 100 [1(a)], 200 [1(b)] and 300 MeV [1(c)] proton and neutron scattering from ^{208}Pb from the Dirac and microscopic Schrödinger models. (Hereafter, for simplicity, we will use the term Schrödinger model as referring to the microscopic Schrödinger model.) The results for proton and neutron scattering calculated from the Schrödinger model are shown by the solid lines, while those from the Dirac model are portrayed by the dashed lines. We first consider the results for 100 MeV scattering. The cross sections for proton scattering as obtained from both models are very similar in shape and magnitude, and agree quite well with the 98 MeV data of Schwandt *et al.* [9]. While the similarity between the two models is also observed for neutron scattering, the level of agreement worsens above 20° , although both models predict a lack of structure in this angular region compared to the proton scattering results. The results of the Schrödinger model calculations reproduce the 200 MeV data of Hutcheon *et al.* [10] well, but not so well for the 300 MeV case. This energy is currently the upper limit for the nonrelativistic microscopic formalism using a bare NN potential. The underlying NN potential must account for particle production at 300 MeV and higher as each nucleon resonance is excited before agreement in the nucleon-nucleus scattering may be achieved. This may account for the disagreement in magnitude between the two models in the neutron scattering at 300 MeV. Over all energies for both projectiles, however, the agreement in the calculated differential elastic scattering from the two approaches is surprisingly good.

As already stated, Kozack and Madland [6] observed a striking phenomenon in the analyzing powers for 100 MeV nucleon- ^{208}Pb elastic scattering. In that work, they noticed that the proton and neutron scattering analyzing powers were out of phase, and the one

almost the inverse of the other about their mean, with the neutrons exhibiting a high polarization above 20° (Fig. 3 of [6]). (A detailed investigation of this phenomenon is outside the scope of this Letter, but work in progress indicates the dominant element to be the presence or absence of a strong Coulomb field.) We compare the results for the analyzing powers at 100, 200, and 300 MeV from the Schrödinger and Dirac models in Fig. 2. In Fig. 2(a), one observes immediately that the same phenomenon as observed by Kozack and Madland is reproduced by the Schrödinger model, although the peaks are more exaggerated than in the Dirac results. Note that both models reproduce the 98 MeV data of Schwandt *et al.* [9]. The phenomenon is explicitly illustrated in Fig. 3, which displays the spin observables for 100 MeV scattering. Both the Dirac and Schrödinger models predict the effect. A significant difference between the 100 MeV proton and neutron scattering spin rotations is also observed with both models, though not as dramatic as that between the analyzing powers. Their similarity again gives confidence in the results obtained from both models and we encourage measurements of these spin observables, especially the analyzing powers, to see if this is a real effect. Such a measurement would also serve to assess the models, especially for neutron scattering. We note here that neither model has yet explicitly included Mott-Schwinger scattering, but that would be the next step especially if contrary experimental evidence appears. The 200 and 300 MeV results are less striking in the proton and neutron analyzing power differences and beyond 15° the proton and neutron analyzing powers are similar for both energies. Significant differences are observed only in the forward angle scattering, especially at 300 MeV, where in both models the minimum at 8° in the neutron scattering analyzing power is missing in that for proton scattering. Again, the agreement between the two models, especially in this spin observable, is much better than had been expected. Note that the 200 MeV proton scattering data were used in the global least-squares adjustment to determine the Dirac optical potential at that energy, and so the level of agreement between those data and the Dirac result is to be expected. The Schrödinger 200 MeV proton result is a prediction.

The dramatic difference in the analyzing power at 100 MeV is also seen in the spin rotation function, displayed in Fig. 4. As with the other two observables, the relative features between the proton and neutron scattering results at all three energies are common to both models. However, the variations in the neutron scattering results from the two models are more distinct at 100 MeV, and less so as one increases the energy. At 200 MeV, the agreement between the Dirac model and the data of Hutcheon *et al.* [10] again is quite good. While that level of agreement is not obtained with the Schrödinger model that calculation reproduces most of the features in the data. As with the analyzing powers at 200 and 300 MeV, the differences between the proton and neutron spin rotation functions from both models significantly differ only below 20° . Thus, the two model approaches are in good agreement for both spin observables for both projectiles in their similarities as well as in their differences.

Fundamentally, our Dirac and Schrödinger approaches are different. That the two models agree so well for the differential cross sections as well as both spin observables for both projectiles not only gives confidence in the calculated results at the three energies considered but also suggests, rather strongly, that the models are physically equivalent over this energy range. Namely, the microscopic Schrödinger model incorporates all the dominant medium modifications in the optical potential without significant approximation by using a realistic

ground state density yielding a reasonable specification of all terms in the optical potential, whereas the Dirac approach provides for a natural specification of such terms. The comparison obtained in this work is exemplary of the dilemma in judging the relative merits of relativistic *vs.* nonrelativistic approaches in intermediate energy proton-nucleus scattering analyses [1]. As Ref. [1] speculates, the answer throughout the energy regime may lie in QCD-based models of nuclear scattering systems. Such theoretical models and concomitant experiments will require simultaneous treatment of proton and neutron scattering in order to be complete; the latter's experimental database is currently sadly lacking. Finally, the question remains: is the difference between the proton and neutron analyzing powers at 100 MeV real? Only experiment will provide the final answer to that question.

This work was supported by the United States Department of Energy Contract no. W-7405-ENG-36. It is dedicated to the memory of Richard Kozack.

REFERENCES

- [1] L. Ray, G. W. Hoffmann, and W. R. Coker, Phys. Rep. 212 (1992) 223, and references cited therein.
- [2] K. Amos, P. J. Dortmans, H. V. von Geramb, S. Karataglidis, and J. Raynal, Adv. Nucl. Phys. 25 (2000) 275.
- [3] R. Kozack and D. G. Madland, Phys. Rev. C 30 (1989) 1461.
- [4] R. Kozack and D. G. Madland, Nucl. Phys. A 552 (1993) 469.
- [5] P. K. Deb, K. Amos, S. Karataglidis, M. B. Chadwick, and D. G. Madland, Phys. Rev. Lett. 86 (2001) 3248.
- [6] R. Kozack and D. G. Madland, Nucl. Phys. A 509 (1990) 664.
- [7] B. D. Serot and J. D. Walecka, Adv. Nucl. Phys. 16 (1986) 1.
- [8] B. C. Clark *et al.*, Phys. Rev. C 30 (1984) 314.
- [9] P. Schwandt *et al.*, Phys. Rev. C 26 (1982) 55; P. Schwandt, private communication, 1996.
- [10] D. A. Hutcheon *et al.*, Nucl. Phys. A 483 (1988) 429.
- [11] R. Machleidt, K. Holinde, and Ch. Elster, Phys. Rep. 149 (1987) 1.
- [12] J. Raynal, computer code DWBA98, NEA 1209/05, 1999.
- [13] B. A. Brown, Phys. Rev. Lett. 85 (2000) 5296.

FIGURES

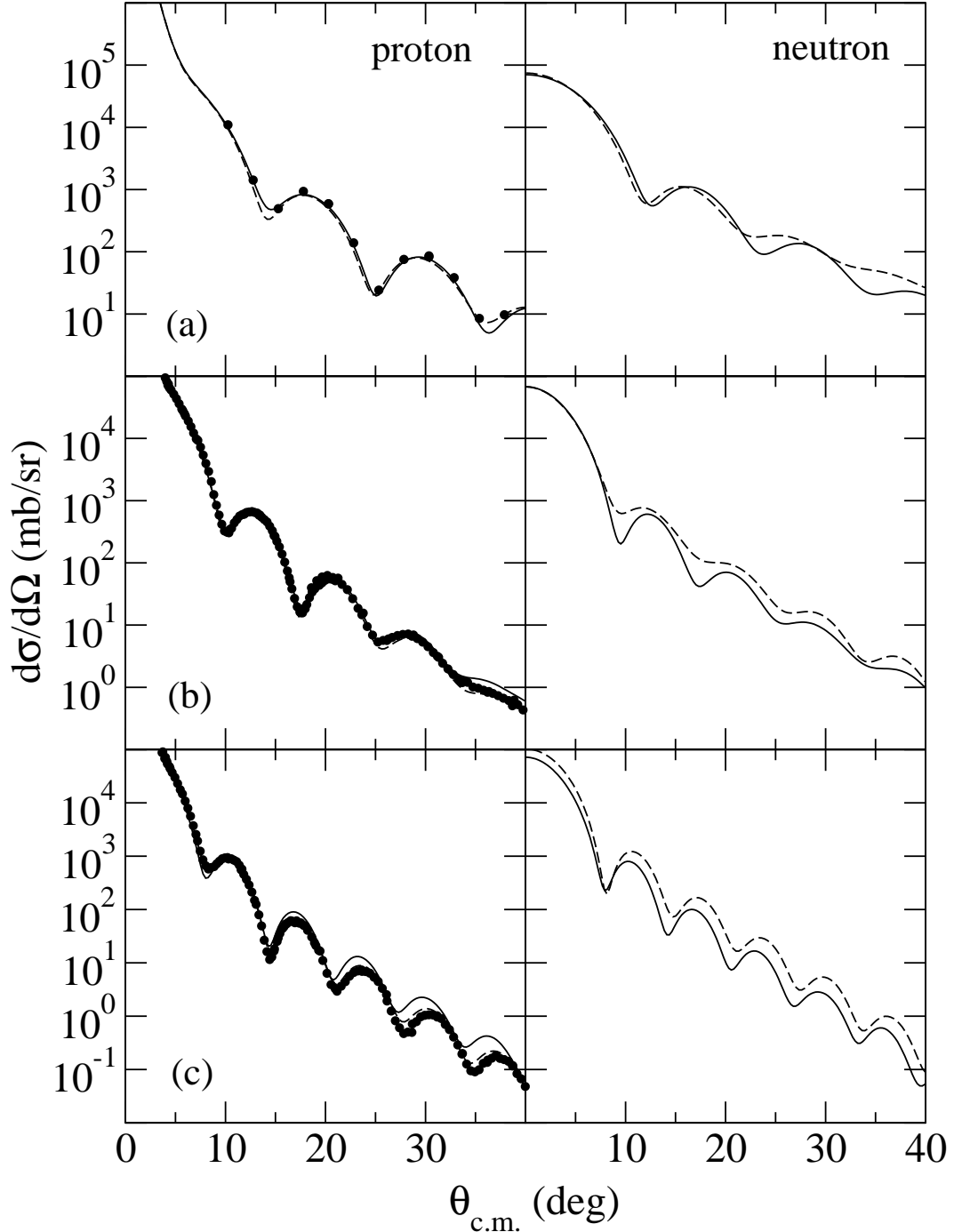


FIG. 1. Differential cross sections for nucleon- ^{208}Pb elastic scattering at 100 (a), 200 (b) and 300 MeV (c). The results for proton and neutron scattering calculated from the Schrödinger model are shown by the solid lines while the results from the Dirac model are shown by the dashed lines. The 100 MeV results are compared to the 98 MeV proton scattering data of Schwandt *et al.* [9]. The 200 and 300 MeV proton scattering data are those of Hutcheon *et al.* [10].

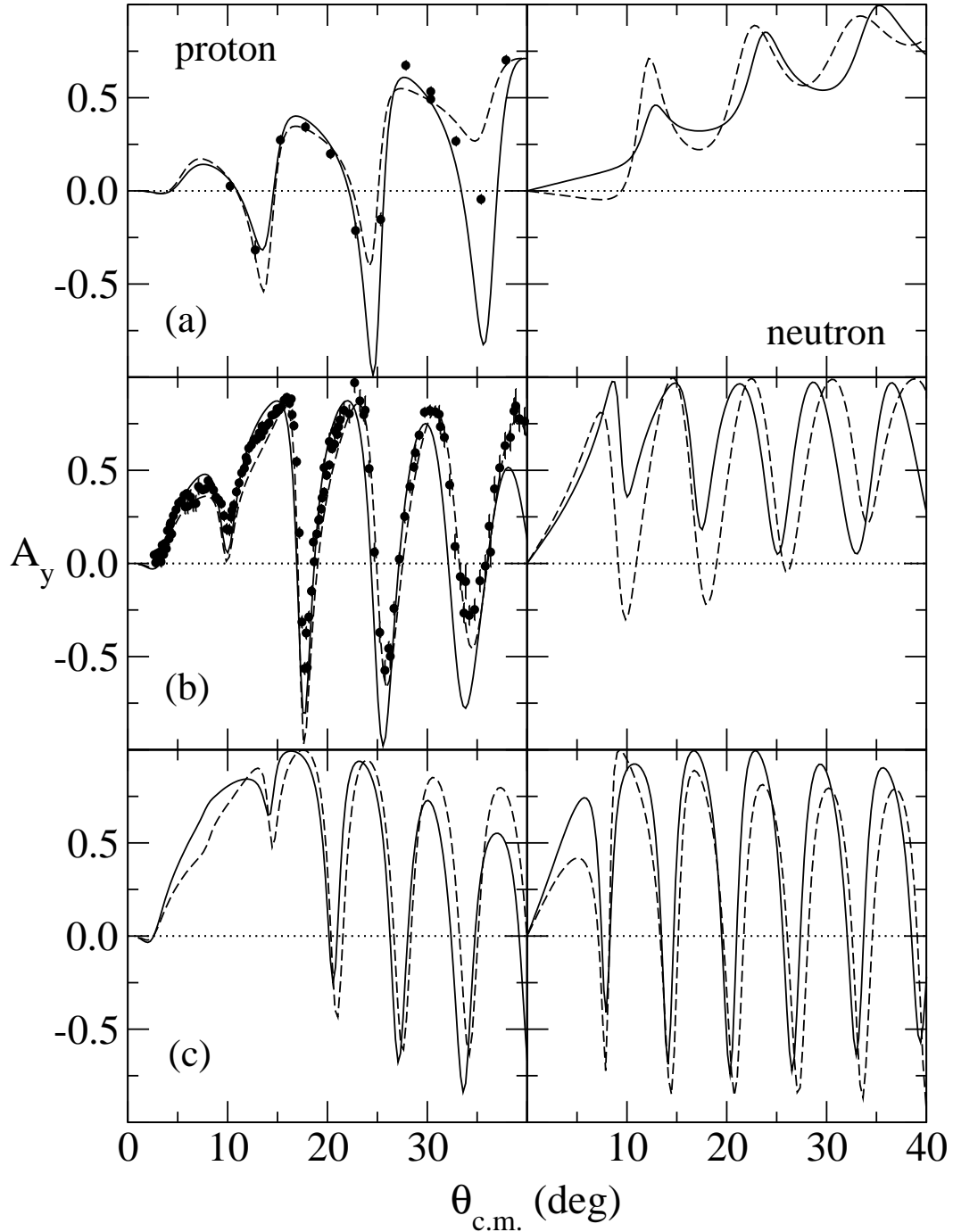


FIG. 2. As for Fig. 1, but for the analyzing powers. The 100 MeV results are compared to the 98 MeV proton scattering data of Schwandt *et al.* [9]. The 200 MeV proton scattering data are those of Hutcheon *et al.* [10].

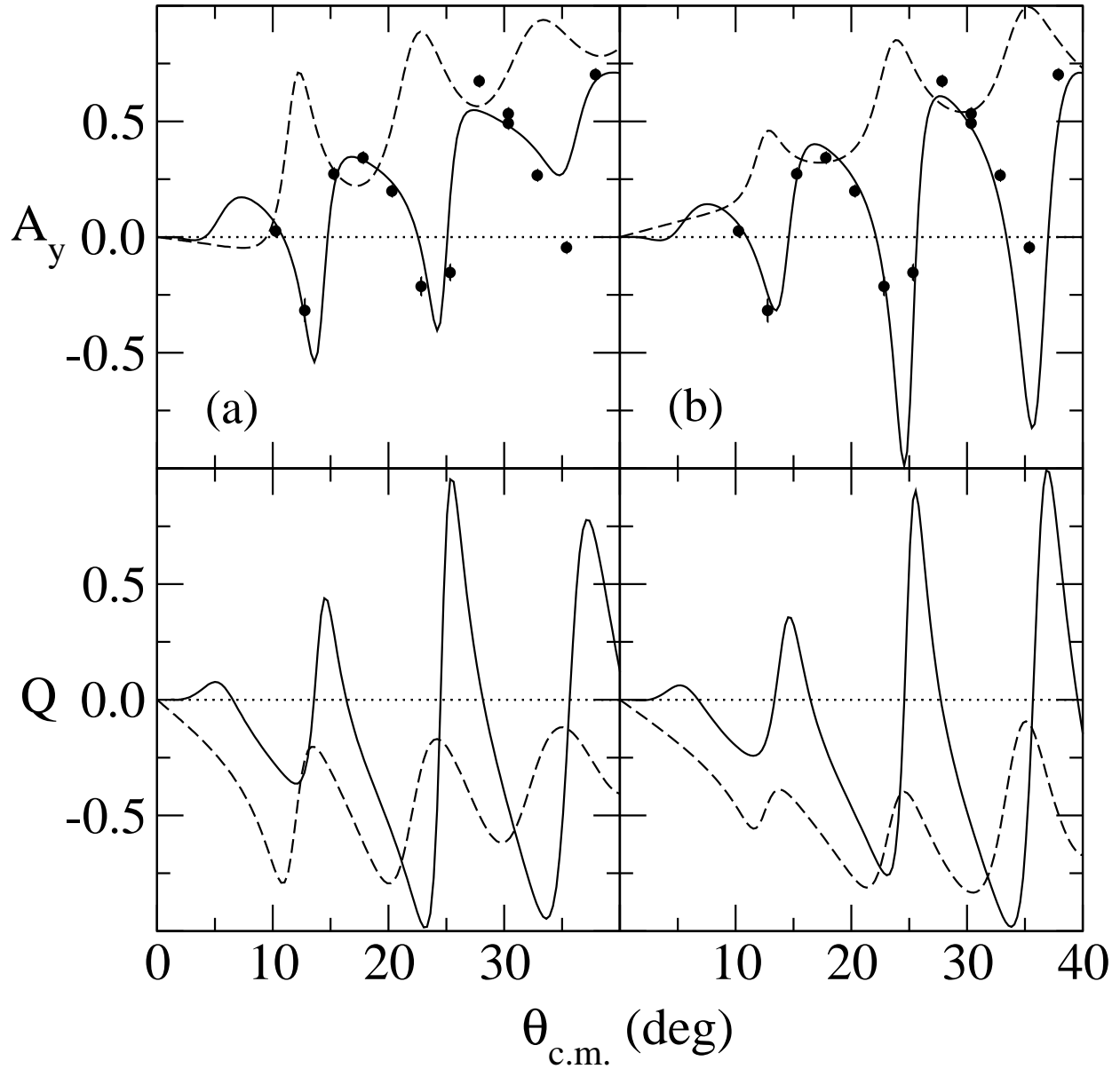


FIG. 3. Analyzing power and spin rotation for the scattering of 100 MeV nucleons from ^{208}Pb . The Dirac and Schrödinger results are displayed in (a) and (b), respectively, while the proton and neutron scattering results are portrayed by the solid and dashed lines, respectively. The proton scattering results are compared to the 98 MeV data of Schwandt *et al.* [9].

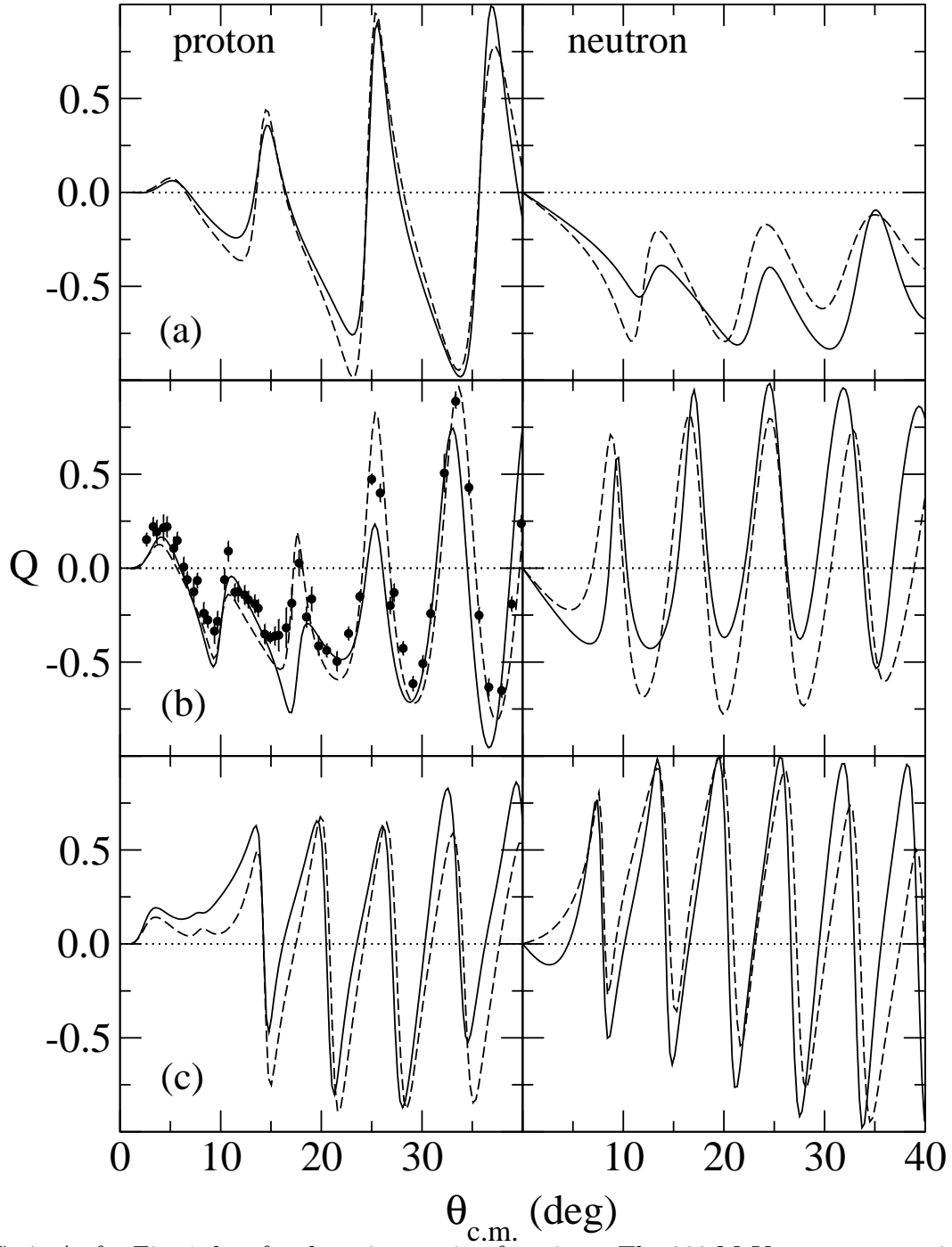


FIG. 4. As for Fig. 1, but for the spin rotation functions. The 200 MeV proton scattering data are those of Hutcheon *et al.* [10].